JOURNAL OF OPTOELECTRONICS AND ADVANCED MATERIALS Vol. 21, No. 11-12, November – December 2019, p. 710 - 716

Ultrafast laser plasma doping of Er^{3+} in Si_3N_4-on-silicon

S. A. KAMIL[a,*], J. CHANDRAPPAN[b], T. F. KRAUSS[c], G. JOSE[d]
[a]*Faculty of Applied Sciences, Universiti Teknologi Mara, 40450 Shah Alam, Selangor, Malaysia*
[b]*Centre for Process Innovation Limited (CPI), Neville Hamlin Building, NETPark, Thomas Wright Way, Sedgefield, County Durham, TS21 3FG, United Kingdom*
[c]*Department of Physics, University of York, York, YO10 5DD, United Kingdom*
[d]*Applied Photon Science, School of Chemical and Process Engineering, University of Leeds, Leeds LS2 9JT, United Kingdom*

An ultrafast laser plasma doping (ULPD) technique is used to dope Er^{3+} into silicon nitride (Si_3N_4)-on-silicon substrate. An adjustable refractive index (1.9-2.9) makes silicon nitride a highly suitable candidate for erbium-doped waveguide amplifier (EDWA) applications. The resultant layers consist of a mixture of target glass with Si_3N_4 and the structural and optical properties are varied according to fs-laser energy used. The use of higher fs-laser energy caused the formation of a thicker doped layer on Si_3N_4, predominantly with target material elements. However, surface doped layers were rougher when higher fs-laser energies were used. The doped layer exhibits spectroscopic characteristics of erbium with photoluminescence lifetimes varying from 3.95 to 9.59 ms.

(Received January 14, 2019; accepted December 10, 2019)

Keywords: Ultrafast lasers, Laser ablation, Optical materials, Er^{3+}-doped glasses

1. Introduction

Recently, photonic integrated circuit (PIC) technology is thriving and in high demands for high-speed data transmission. The advantages of this technology are wide bandwidth, small size, lightweight and low power consumption. PICs consists of functional photonic components such as an optical filter, laser, waveguide arrays, splitters, modulator, and photodetector [1]. However, as the number of PIC components increases, the associated inherent loss due to propagation and interconnects also increases. An integrated optical amplifier (OA) can boost the signal to mitigate such losses associated with dense integrations. Due to the high demands for greater bandwidth and to go with the ever-increasing need for speed in all aspects of society, industry and business, this, in turn, requires smaller and more efficient integrated optical amplifiers.

Among the available optical OAs, erbium-doped waveguide amplifier (EDWA) could be potentially used in PIC due to its advantages over other OAs such as semiconductor optical amplifier (SOA) and erbium-doped fiber amplifier (EDFA). The drawbacks of SOA is that it has a high noise, polarization dependence and high cross-talk [2,3]. Although EDFA has better performance than SOA, its bulky structure makes the packaging become expensive and hindrance for a miniature device. To overcome this, the concept of erbium-doped waveguide amplifier (EDWA) was introduced, and its fundamental operation is similar to an EDFA but with a smaller size.

In the past few years, numerous research was done to realise an EDWA in various materials systems such as glass, ceramics and polymers. A high refractive index for EDWA is preferred as it supports the miniaturisation of OA to meet the emerging demands [4]. Waveguide that has a high refractive index is required because it can confine light very well within the waveguide core. However, high index cores are more likely to experience surface scattering that can contribute to loss. Since there are many trade-offs when selecting a suitable refractive index, the device designer needs a material that has an adjustable refractive index. Silicon nitride is one of such materials that offer the flexibility to modify refractive index in a wide range (1.9-2.9) [5,6] and this material is compatible with the CMOS silicon processing techniques.

There are a few methods that is reported to prepare Er-doped Si_3N_4 such as ion implantation [7] and RF magnetron reaction sputtering [8]. In the present study, ultrafast laser plasma doping technique (ULPD) was employed to dope erbium into Si_3N_4. This technique has been proven effective for doping erbium into silica [4,9] by using femtosecond (fs) laser to ablate target glass and generates highly energetic plasma. The plasma plume that consists elements from target glass then interact and integrate with substrate. The resulting layer properties were highly dependent on the process parameters used. Here, various fs-laser energies were utilized to study its effect on the doped layer.

2. Experimental details

2.1. Target glass preparation

$79.5TeO_2$-$10ZnO$-$10Na_2O$-$0.5Er_2O_3$ (Er-TZN) was fabricated using analytical grade chemicals (TeO_2, ZnO, Na_2O and Er_2O_3) with an initial purity of higher than 99.99%. It was prepared by using a standard melt-quenching technique [10]. The resulting target glass was

then polished using a polishing machine (Buehler, Motopol, 2000) with various grades of silicon carbide paper (Buehler Grit P1200, P2400, and P4000) in order to obtain an optically smooth and flat surface.

2.2. Ablation experiments

The clean Si_3N_4 (1 μm)-on-silicon substrate was heated at a temperature of 570 ℃ and was placed 70 mm above the target. Target glass was ablated by a commercial Coherent Ti: Sapphire LIBRA laser (pulse duration of 100 fs, wavelength of 800 nm and pulse repetition rate of 1 kHz) with different fs-laser energy (30, 40, 50, 60 and 80 μJ). The fs-laser energy was adjusted by a beam splitting polariser and half-wave plate and the energies were determined with a pyroelectric detector and energy meter (PE50-DIF-C and Starlite Energy Meter, Ophir). The ablations process was performed in a vacuum chamber for four hours under an oxygen ambient of 70 mTorr.

2.3. Characterisation

A bare Si_3N_4 substrate and five samples prepared were characterized by a Hitachi SU8230 scanning electron microscope (SEM) and energy dispersive X-ray (EDX) in order to determine the cross-section morphology and the elemental concentration in the sample, respectively. X-ray diffraction (XRD) (Philips X'Pert) was employed to determine the crystallinity of the processed layer. Raman spectra of the samples were recorded by Renishaw inVia micro at room temperature using the 514 nm excitation wavelength with a power of 25 mW. Photoluminescence (PL) emission spectra were collected using a spectrometer (Edinburgh Instruments FLS920 series) with a 980 nm laser as the excitation source. PL lifetime measurement was also carried out using time-resolved PL spectra (laser source which was pulsed using a 100-ms period and a pulse width of 10 μs).

3. Results and discussions

Five samples were labelled according to the fs-laser energy used for the fabrication. Sample N30 represents the sample fabricated with 30 μJ laser energy whilst the higher fs-laser energy at 40, 50, 60 and 80 μJ are labelled with codes N40, N50, N60, and N80, respectively. Fig. 1(a) presents a backscattered (BSE) cross-section SEM image for Si_3N_4 (1 μm)-on-silicon substrate while Fig. 1(b) – 1(f) displays the images for samples doped with Er-TZN by using various fs-laser energies. The elemental composition for several positions in the doped layer for sample N30 and N50 were provided in Table 1. It is observed that the doped layer consists of combination of elements from the target glass and Si_3N_4 substrate. It appears that cations such as Te, Zn, Na and Er were removed from the target glass and penetrated the substrate and modified the host Si_3N_4 network.

Surprisingly, the concentration of N in the doped layer for N50 was very low, compared to its concentration in Si_3N_4. It is assumed that nitrogen is lost in the form of nitrogen gas when the tellurite glass reacted with Si_3N_4, which is also reported by Watanabe et al [11]. Although elements from target glass managed to penetrate the Si_3N_4, it is discretely distributed as depicted by the grayscale variations in the doped layers (Fig. 1(b) – 1(f)). This largely inhomogeneous layer appeared to be partly porous, and in certain areas, there is an accumulation of specific elements. An area scan (Fig. 2) was carried out to view the entire elemental distribution present in the doped layer. Interestingly, it is discovered that the Te had an even distribution over the entire doped layer. The area scan for Er is less obvious because of its very low concentration, resulting in a lot of noise in the scan results. On the other hand, for sample N30, it is found that very few Er-TZN elements managed to penetrate into the Si_3N_4. The upper layer still has a plenty of nitrogen species, and this proves that at fs-laser energy of 30 μJ, species in the Er-TZN are unable to interact efficiently with the Si_3N_4 network due to species in the plasma plume having low kinetic energy and velocity.

In addition, lower energy ablation using fs-laser energies of 30 and 40 μJ led to a more uniform layer and particle size reduction (Fig. 1(b)-1(c)). This is because higher fs-laser energy caused the plasma plume to be denser and enhanced the molecular interactions that led to the formation of bigger particles [12]. Furthermore, when higher fs-laser energy is used on the target material, the absorption depth becomes larger, and this could lead to superheating of a large volume. As a result of this heating process, the volume could transform into the melt phase due to rapid expansion thus increasing the number of molten droplets or particulates ejected from the target [13].

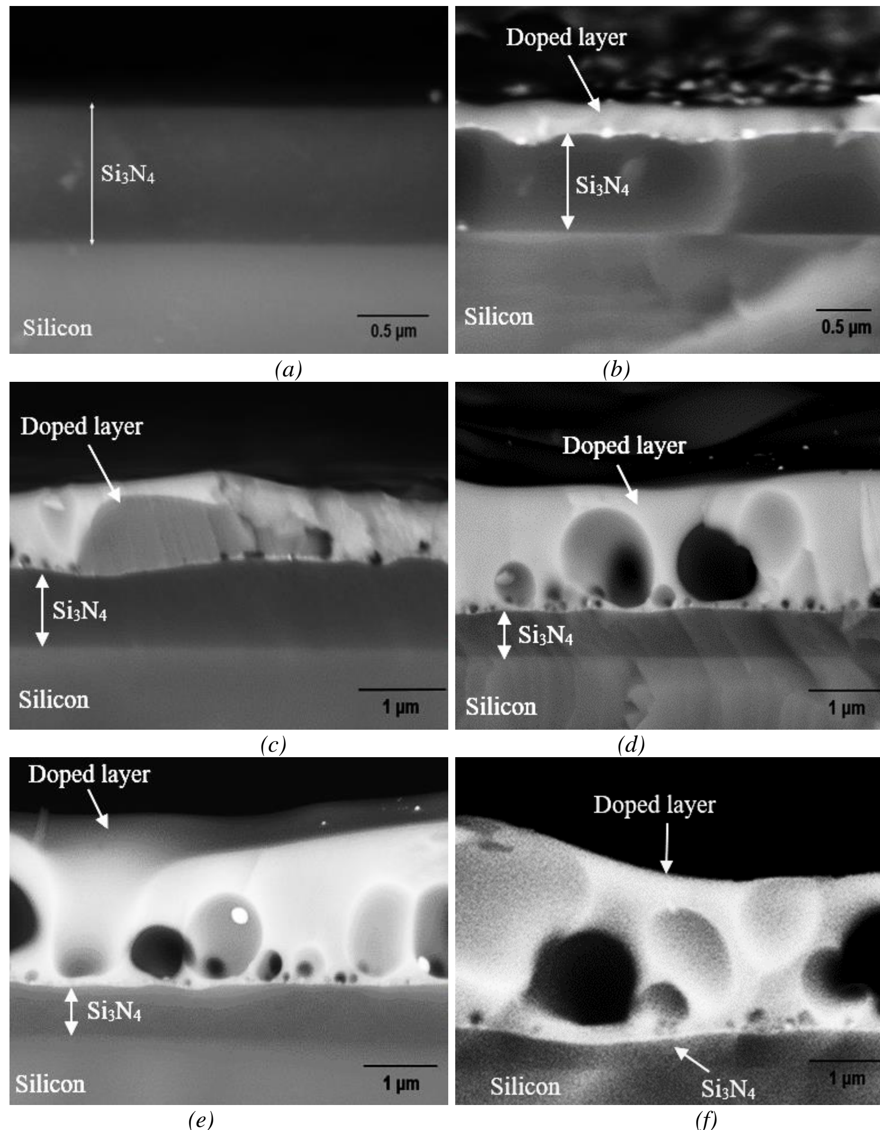

Fig. 1. Backscattered cross-section SEM image of (a) Si_3N_4-on-silicon substrate and samples doped with Er-TZN using fs-laser energy of (b) 30 µJ (N30) (c) 40 µJ (N40) (d) 50 µJ (N50) (e) 60 µJ (N60) and (f) 80 µJ (N80).

The thicknesses of the doped layers for all the samples are summarised in Table 2. The doped layers were found to be higher with increased fs-laser energy from the SEM images (Fig. 1(b) – 1(f)). This increment was due to a higher incident ion flux from the laser-produced plasma at higher energies. The pristine Si_3N_4 layer decreased as a result of modification of Si_3N_4 surface by the transformation into the doped layer. The very high measurement error for the thickness of sample N80 compared to the other samples indicates that the surface of this sample is very rough. The large particle size that results from the use of high fs-laser energy causes the surface doped layer to be very rough.

Table 1. Elemental concentration of sample N30 and N50 at three different locations[a]

Element	Sample N30			Sample N50		
	Position 1	Position 2	Position 3	Position 1	Position 2	Position 3
O	12.84	12.35	6.59	29.00	34.77	50.52
Si	30.96	31.22	34.24	20.07	28.21	19.05
Te	0.19	0.16	3.15	34.58	14.25	6.91
Zn	1.61	1.46	1.98	5.12	9.78	9.29
Na	2.61	2.53	3.04	8.61	10.35	10.46
Er	0.07	0.10	0.12	1.66	1.41	2.13
N	51.72	52.18	50.88	0.96	1.23	1.64

[a]*The estimated uncertainty is ±0.01 at. %.*

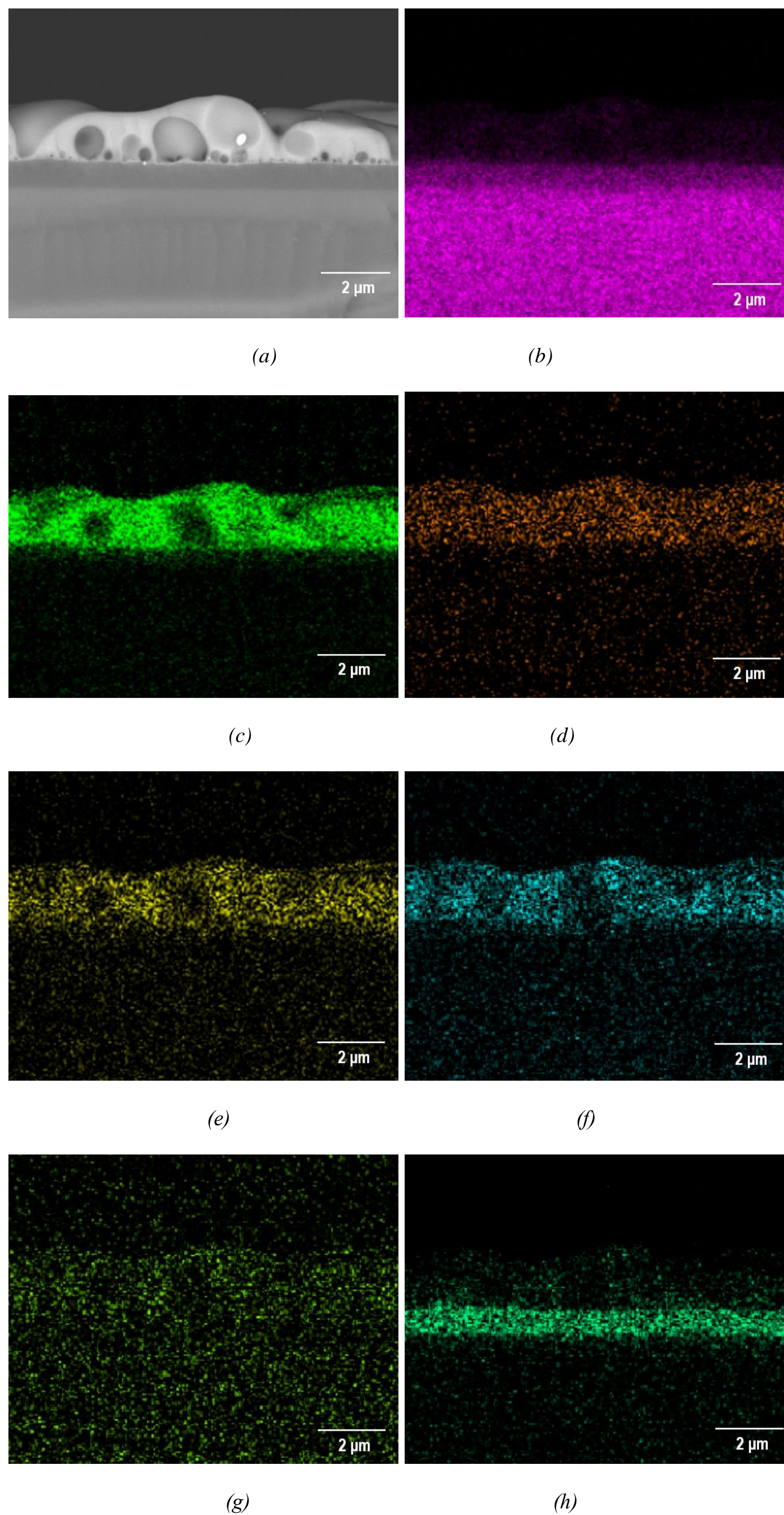

Fig. 2. Area scan measured by EDX-SEM for sample N50 with (a) the area being measured. The distribution of species presents in it which were (b) silicon, (c) oxygen, (d) tellurium, (e) zinc, (f) sodium, (g) erbium and (h) nitrogen

Table 2. Thickness of the upper layer and Si_3N_4 underneath it measured by SEM for samples N30, N40, N50, N60 and N80

Samples	Thickness (μm)	
	Doped layer	Si_3N_4 underdoped layer
N30	0.285 ± 0.053	0.811 ± 0.049
N40	0.870 ± 0.205	0.754 ± 0.136
N50	1.573 ± 0.264	0.596 ± 0.140
N60	2.002 ± 0.293	0.548 ± 0.034
N80	2.313 ± 0.948	0.467 ± 0.066

Fig. 3 displays the XRD patterns of samples N30, N40, N50, N60 and N80. The indexed peaks assigned to the possible crystalline structures are also shown in Fig. 3. The 2θ peak located at approximately ~69° is a crystalline Si (100) peak that originates from the silicon substrate. The peaks at 24.03°, 24.97°, 35.02°, 43.19° and 50.45° are attributed to the $Na_2Zn_3(SiO_4)_2$ (ICCD reference code: 00-012-3700) while two peaks detected at the 2θ angle of 27.87° and 38.63°corresponded to Te (ICCD reference code: 00-036-1452). The increased intensity for the peak of Te when higher laser energy was used indicated that the level of Te clustering increased with fs-laser energy. For sample N30 and N40, there is a SiO_2 intense peak at 21.34° (ICCD reference code: 00-039-1425). The increase of Er-TZN in the doped layer (N50, N60 and N80) caused the crystalline phase SiO_2 disappear, making it more likely to consist of amorphous silicate. The appearance of an halo around 32° for sample N50, N60 and N80 which often associated with amorphous silicate [9,14,15] is the evidence for this. On the other hand, the Si_2N_2O peak at 2θ of 26.32° [16] appeared in the N30 sample, and this clearly showed that there is still a high nitrogen content in this layer as also shown in Table 1.

Fig. 4 shows the Raman spectra of samples N30, N40, N50, N60 and N80. All samples including the substrate reported the peak of the wavelength of 521 cm^{-1} attributed to single-crystalline silicon [17] derived from the substrate. This intensity of this peak appeared to be the lowest for sample N80 because doped layer for this sample is the thickest which, in turn, caused the signal from Si substrate to be weak. There are peaks at the wavenumber of 122 and 141 cm^{-1} that corresponds to metallic tellurium [18,19]. These peaks are lower for the N30 sample compared to the other samples as the amount of Te in N30 was the lowest from others. For peaks located at high wavenumber which are at 1160 and 1544 cm^{-1}, these two peaks are linked with erbium fluorescence emission [20]. However, peaks in the high wavenumber regime appeared to be unclear for sample N30 due to the very small concentration of Er in the sample. A broad peak around 900-1050 cm^{-1} also appeared for sample N30, which is believed to be associated with a Si-O bond, as reported in the literature [21–23].

Fig. 5 illustrates the PL spectra for samples N30, N40, N50, N60 and N80. The PL intensity becomes higher for samples that were prepared with higher laser energy except for the N80 sample. The phenomenon of decreasing PL intensity that was observed for the N80 sample is known as photoluminescence quenching and is due to the very high concentration of erbium in the sample [24,25]. The short distance between Er^{3+}-Er^{3+} triggered this concentration quenching effect, which could have induced energy transfers between them. Otherwise, the very low erbium concentration in the N30 sample caused Er emission to appear very weak. PL lifetime and full half-width maximum (FWHM) for every sample are shown in Table 3. Based on the obtained FWHM, all samples, except for N30 and N40, showed the PL characteristics like erbium-doped silicate glass [9,26]. The broader FWHM for sample N30 and N40 might have been due to its environment host that differed from the other samples due to higher nitrogen content. Sample N30 and N40 had a very low lifetime of 3.95 ms and 5.12 ms, respectively and this low lifetime is probably due to erbium in the silicon oxynitride environment, which is often reported to have a PL lifetime in the range of 0.5-7 ms [27–29]. For the N80 sample, the main network is still silicate based on its FWHM which had a value of 20 nm. However, the drastic decrease of PL lifetime for this sample is due to concentration quenching [25,30].

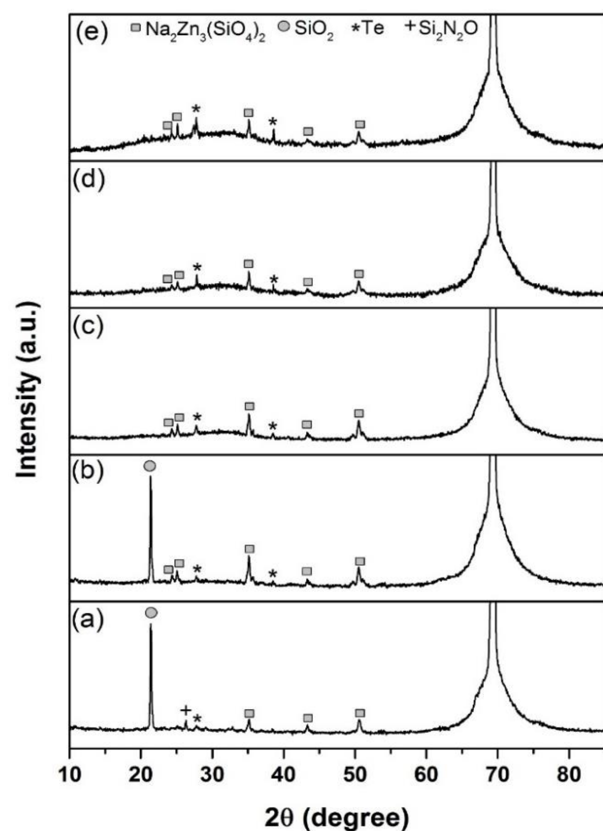

Fig. 3. XRD spectra of doped layer on Si_3N_4-on-silicon fabricated using a fs-laser energy of (a) 30 μJ (N30), (b) 40 μJ (N40), (c) 50 μJ (N50), (d) 60 μJ (N60) and (e) 80 μJ (N80)

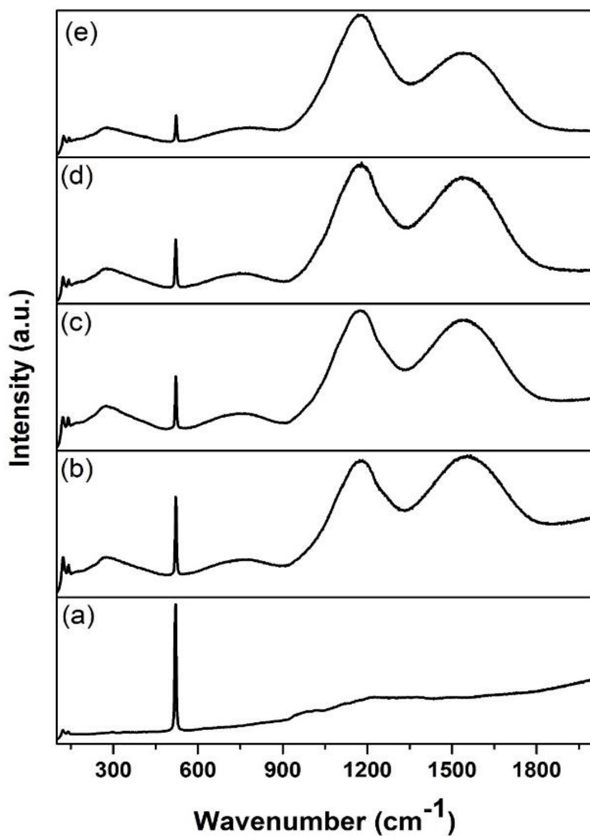

Fig. 4. Raman spectra for sample fabricated using a fs-laser energy of (a) 30 µJ (N30), (b) 40 µJ (N40), (c) 50 µJ (N50), (d) 60 µJ (N60) and (e) 80 µJ (N80)

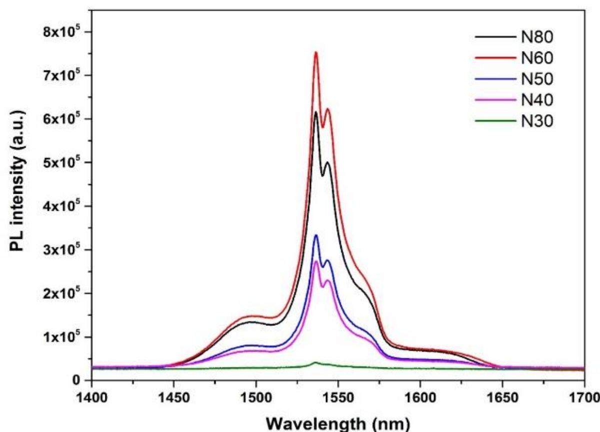

Fig. 5. Room temperature PL spectra of the $^4I_{13/2} \rightarrow {}^4I_{15/2}$ transition of erbium ion for samples N30, N40, N50, N60 and N80

Table 3. PL lifetime and FWHM for doped layer prepared using different laser energies

Samples	PL lifetime (ms)	FWHM (nm)
N30	3.95	25
N40	5.14	23
N50	9.59	20
N60	9.02	20
N80	6.33	20

4. Conclusion

In summary, Er-TZN is integrated with Si_3N_4 network under the ULPD process. The inhomogeneous layer formed is partly porous, and in certain areas, there is an accumulation of specific elements. Nitrogen is lost in the form of nitrogen gas when the tellurite glass reacted with Si_3N_4.

The doped layer thickness and PL lifetime can be controlled by altering the fs-laser energies. The blending of Er-TZN with Si_3N_4 could be improved by altering other different process parameters such as substrate temperature, fs-laser repetition rate, background gas pressure, ablation period and type of background gas.

Acknowledgements

The author would like to state that this work was supported by the Engineering and Physical Sciences Research Council (EPSRC) (EP/M015165/1 and EP/M022854/1).

References

[1] J. Liu, M. Beals, J. Michel, L. C. Kimerling, ECS Trans. **19**, 17 (2009).
[2] I. T. Monroy, E. Tangdiongga, Crosstalk in WDM Communication Networks, Springer, New York (2012).
[3] T. S. El-Bawab, Optical Switching, Springer, New York (2006).
[4] J. Chandrappan, M. Murray, T. Kakkar, P. Petrik, E. Agocs, Z. Zolnai, D. P. Steenson, A. Jha, G. Jose, Sci. Rep. **5**, 14037 (2015).
[5] D. S. Kim, S. G. Yoon, G. E. Jang, S. J. Suh, H. Kim, D. H. Yoon, J. Electroceramics **17**, 315 (2006).
[6] S. Duttagupta, F. Ma, B. Hoex, T. Mueller, A. G. Aberle, Energy Procedia **15**, 78 (2012).
[7] W. C. Ding, D. Hu, J. Zheng, P. Chen, B. W. Cheng, J. Z. Yu, Q. M. Wang, J. Phys. D. Appl. Phys. **41**, 135101 (2008).
[8] W. Ding, Y. Zuo, Y. Zhang, J. Guo, B. Cheng, J. Yu, Q. Wang, H. Guo, P. Lu, J. Shen, J. Semicond. **30**, 102001 (2009).
[9] S. A. Kamil, J. Chandrappan, M. Murray, P. Steenson, T. F. Krauss, and G. Jose, Opt. Lett. **41**, 4684 (2016).
[10] A. Jha, B. D. O. Richards, G. Jose, T. Toney Fernandez, C. J. Hill, J. Lousteau, P. Joshi, Int. Mater. Rev. **57**, 357 (2012).
[11] S. Watanabe, T. Kodera, and T. Ogihara, J. Ceram. Soc. Japan **124**, 218 (2016).
[12] A. Nath, A. Khare, in Laser Ablation Liquids: Principles and Appllications in the Prepation of Nanomaterials, edited by G. Yang (Pan Stanford Publishing, Temasek Boulevard, 2012), p. 947.

[13] S. Bar, Crystalline Rare Earth Doped Sesquioxide PLD-Films on A-Alumina: Preparation and Characterization, University of Hamburg, 2004.
[14] H. Zhang, J.-H. Zhou, Q.-L. Zhang, H. Yang, J. Inorg. Mater. **28**, 785 (2013).
[15] X. Kang, S. Huang, P. Yang, P. Ma, D. Yang, J. Lin, Dalton Trans. **40**, 1873 (2011).
[16] S. Wu, X. Li, Int. J. Refract. Met. Hard Mater. **36**, 97 (2013).
[17] T. Seuthe, M. Grehn, A. Mermillod-Blondin, H. J. Eichler, J. Bonse, M. Eberstein, Opt. Mater. Express **3**, 755 (2013).
[18] W. D. Bonificio, D. R. Clarke, J. Appl. Microbiol. **117**, 1293 (2014).
[19] Y. C. Her, S. L. Huang, Nanotechnology **24**, 215603 (2013).
[20] J. Cui, G. A. Hope, J. Spectrosc. **2015**, 940172 (2015).
[21] L. Robinet, C. Coupry, K. Eremin, C. Hall, J. Raman Spectrosc. **37**, 789 (2006).
[22] K. Bourhis, Y. Shpotyuk, J. Massera, V. Aallos, T. Jouan, C. Boussard-plédel, B. Bureau, L. Petit, J. Koponen, L. Hupa, M. Hupa, and M. Ferraris, Opt. Mater. (Amst). **37**, 87 (2014).
[23] C. Calahoo, J. W. Zwanziger, I. S. Butler, J. Phys. Chem. C **120**, 7213 (2016).
[24] Y.-L. Lu, Y.-Q. Lu, N.-B. Ming, Appl. Phys. B **62**, 287 (1996).
[25] S. Dai, C. Yu, G. Zhou, J. Zhang, G. Wang, L. Hu, J. Lumin. **117**, 39 (2006).
[26] A. Polman, Appl. Phys. Rev. **82**, 1 (1997).
[27] A. Pal, P. Saini, S. Sapra, in Fundamentals of Conjugated Polymer Blends, Copolymers and Composites: Synthesis, Properties and Applications, edited by P. Saini (John Wiley & Sons, New Jersey, 2015), p. 163.
[28] S. Saini, Gain Efficient Waveguide Optical Amplifiers for Gain Efficient Waveguide Optical Amplifiers for Si Microphotonics, Massachusetts Institute of Technology, 2004.
[29] J. G. Sandland, Sputtered Silicon Oxynitride for Microphotonics: A Materials Study, Massachusetts Institute of Technology, 1999.
[30] W. J. Miniscalco, in Rare-Earth-Doped Fiber Lasers and Amplifiers, edited by M. J. F. Digonnet (Marcel Dekker, New York, 2001), p. 18.

*Corresponding author: suraya_ak@uitm.edu.my